

Analysis of Finite Field Spreading for Multiple-Access Channel

Guanghai Song, *Student Member, IEEE*, Yuta Tsujii, *Student Member, IEEE*,
Jun Cheng, *Member, IEEE*, and Yoichiro Watanabe, *Member, IEEE*

Abstract

Finite field spreading scheme is proposed for a synchronous multiple-access channel with Gaussian noise and equal-power users. For each user, s information bits are spread *jointly* into a length- sL vector by L multiplications on $\text{GF}(2^s)$. Thus, each information bit is dispersed into sL transmitted symbols, and the finite field despreading (FF-DES) of each bit can take advantage of sL independent receiving observations. To show the performance gain of joint spreading quantitatively, an extrinsic information transfer (EXIT) function analysis of the FF-DES is given. It shows that the asymptotic slope of this EXIT function increases as s increases and is in fact the absolute slope of the bit error rate (BER) curve at the low BER region. This means that by increasing the length s of information bits for joint spreading, a larger absolute slope of the BER curve is achieved. For $s, L \geq 2$, the BER curve of the finite field spreading has a larger absolute slope than that of the single-user transmission with BPSK modulation.

Index Terms

finite field spreading, EXIT function, multiple-access channel, CDMA, IDMA

I. INTRODUCTION

In a K -user multiple-access channel (MAC), each user regards the signals of other users as interference. When the number of users K is large, each user has a very low signal-to-interference-and-noise ratio (SINR) [1]. For this reason, spreading is usually employed as an SINR amplifier for each user, such as the conventional code-division multiple-access (CDMA) [2] and interleave-division multiple-access (IDMA) systems [3]–[6].

In the CDMA and IDMA systems, each information bit is spread *independently*. Specifically, in the CDMA system each information bit is spread by multiplying a binary vector into a length- L bit-vector, which is then interleaved by a bit-level interleaver. Since each

information bit has L independent receiving observations, the despreading (DES) will output an ameliorated signal with a sufficient large SINR for a further outer decoding (if there is a channel code as an outer code). In the IDMA system, a chip-level interleaving is jointly performed on multiple bit-vectors instead of the bit-level interleaving in the CDMA system [4]. As the number of bit-vectors for interleaving is large, the IDMA in fact becomes a multi-user sparse-graph code that is appropriate for iterative decoding [6]. For this reason, the IDMA under an iterative chip-by-chip decoding provides a lower bit error rate (BER) than the conventional CDMA [3] [6]. Simulations in [3] showed that at the low BER region, the BER of the uncoded IDMA system can converge to that of single-user transmission with BPSK modulation. The BER of single-user transmission with BPSK modulation is the performance upper bound for both of the CDMA and IDMA systems, since in both systems the independent spreading of each information bit implies that each user employs a repetition code.

In this paper, we propose a finite field spreading scheme for a synchronous MAC with Gaussian noise and equal-power users. For each user, every s information bits are spread *jointly* into a length- sL vector by L multiplications on $\text{GF}(2^s)$. A chip-level interleaving is then performed to generate the transmitted vector to the MAC. At the receiver, a multi-user iterative decoding is performed on a single factor graph to recover the information vector of each user. In our scheme, due to the joint spreading, each information bit is dispersed into sL transmitted symbols, and the finite field despreading (FF-DES) of each bit can take advantage of sL independent receiving observations. To show the performance gain of joint spreading quantitatively, we analyze the extrinsic information transfer (EXIT) function of the FF-DES. We show that the asymptotic slope of this EXIT function increases as s increases and is in fact the absolute slope of the BER curve at the low BER region. This means that by increasing the length s of information bits for joint spreading, a larger absolute slope of the BER curve is achieved. For $s, L \geq 2$, the BER curve of the finite field spreading has a larger absolute slope than that of the single-user transmission with BPSK modulation.

II. TRANSMITTER MODEL

Figure 1 illustrates a block diagram of the transmitter of K -user finite field spreading multiple-access system. The length- sN information vector $\mathbf{u}^{(k)} = (u_1^{(k)}, u_2^{(k)}, \dots, u_{sN}^{(k)})$, $u_i^{(k)} \in \{+1, -1\} \triangleq \mathcal{X}$, $1 \leq k \leq K$, of user k is first mapped into a length- N vector $\boldsymbol{\beta}^{(k)} = (\beta_1^{(k)}, \beta_2^{(k)}, \dots, \beta_N^{(k)})$ over $\text{GF}(2^s)$, i.e., every s information bits are mapped into a field element by mapping

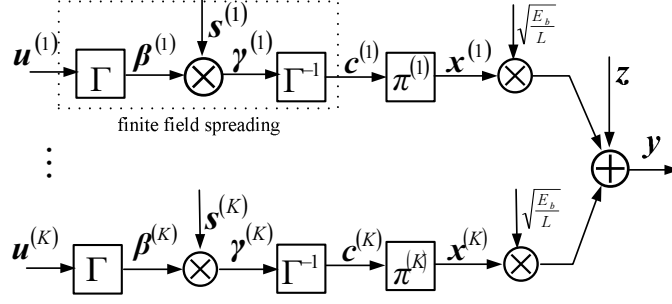


Fig. 1. Transmitter of K -user finite field spreading multiple-access system.

$\Gamma : \mathcal{X}^s \rightarrow \text{GF}(2^s)$. Here $\text{GF}(2^s) = \{0, 1, \alpha, \dots, \alpha^{2^s-2}\}$ is a finite field with a primitive element α , and Γ can be an arbitrary bijection from \mathcal{X}^s to $\text{GF}(2^s)$. Each element $\beta_j^{(k)}$, $1 \leq j \leq N$, in $\boldsymbol{\beta}^{(k)}$ is spread by length- L spreading vector $\mathbf{s}^{(k)}$ over $\text{GF}(2^s)$ into $\beta_j^{(k)} \mathbf{s}^{(k)} = (\beta_j^{(k)} s_1^{(k)}, \beta_j^{(k)} s_2^{(k)}, \dots, \beta_j^{(k)} s_L^{(k)})$, where the multiplication is on $\text{GF}(2^s)$. Here $\mathbf{s}^{(k)}$ can be an arbitrary vector over $\text{GF}(2^s)$ with $s_\ell^{(k)} \neq 0$, $\ell = 1, 2, \dots, L$. The output field vector after multiplication, denoted as $\boldsymbol{\gamma}^{(k)} = (\gamma_1^{(k)}, \gamma_2^{(k)}, \dots, \gamma_{NL}^{(k)})$, is demapped into binary vector $\mathbf{c}^{(k)} = (c_1^{(k)}, c_2^{(k)}, \dots, c_{sNL}^{(k)})$, i.e., each field element is demapped into s bits by demapping $\Gamma^{-1} : \text{GF}(2^s) \rightarrow \mathcal{X}^s$, where Γ^{-1} is the inverse transform of Γ . Vector $\mathbf{c}^{(k)}$, referred to as chip vector, is interleaved by a length- sNL chip-level interleaver $\pi^{(k)}$ and is multiplied by amplitude $\sqrt{\frac{E_b}{L}}$ to generate the transmitted vector $\sqrt{\frac{E_b}{L}} \mathbf{x}^{(k)} = (\sqrt{\frac{E_b}{L}} x_1^{(k)}, \sqrt{\frac{E_b}{L}} x_2^{(k)}, \dots, \sqrt{\frac{E_b}{L}} x_{sNL}^{(k)})$, $x_t^{(k)} \in \mathcal{X}$, to the Gaussian MAC. Here E_b is the energy per information bit, and $\frac{E_b}{L}$ is the symbol energy per transmission due to code rate $\frac{1}{L}$ of each user. The chip-level interleaving should be different for each user as in the IDMA system [3]–[6].

The receiver receives a superimposed signal vector $\mathbf{y} = (y_1, y_2, \dots, y_{sNL})$ with

$$y_t = \sum_{k=1}^K \sqrt{\frac{E_b}{L}} x_t^{(k)} + z_t, \quad t = 1, 2, \dots, sNL \quad (1)$$

where z_t is a zero-mean Gaussian variable with one-side power spectral density N_0 . Here, we assume that the symbols from the K users are synchronous. An iterative multi-user decoding is performed to recover information vectors $\mathbf{u}^{(k)}$, $k = 1, \dots, K$.

To simplify the description, the mapping, multiplication of spreading vector, and demapping in the dotted box in Fig. 1 is referred to as finite field spreading. It should be noted that by the finite field spreading over $\text{GF}(2^s)$, the spreading of s information bits is performed jointly, and each information bit is dispersed into sL transmitted symbols. Thus, the FF-DES of each information bit can take advantage of sL independent receiving observations.

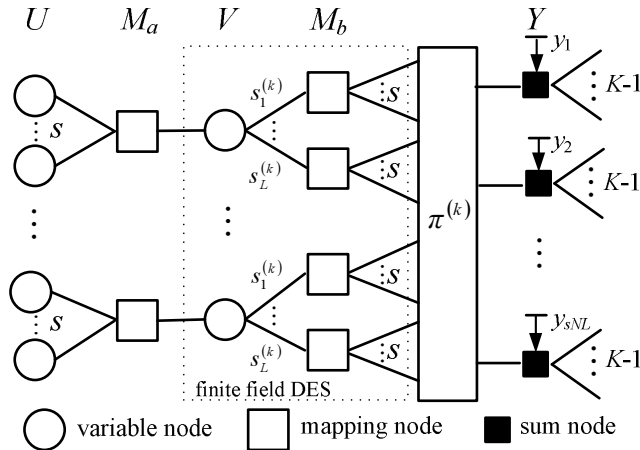


Fig. 2. Factor graph of the finite field spreading and the MAC for user k .

Conventional spreading schemes, such as the CDMA and IDMA where the information bit is spread independently, are special cases of the finite field spreading with $s = 1$.

III. ITERATIVE DECODING ON FACTOR GRAPH

Due to the chip-level interleaving, as length N is large, the K -user finite field spreading multiple-access can be regarded as a K -user sparse-graph code which can be decoded iteratively on a single factor graph. In this section, we give an iterative decoding algorithm of the finite field spreading multiple-access on a single factor graph. In Section III-A, we represent the K -user finite field spreading and the MAC by a single factor graph. In Section III-B, we give the iterative decoding algorithm.

A. Factor Graph

Since each user has the same encoding process, the factor graph of each user is the same. We only illustrate the factor graph of user k in Fig. 2. There are three kinds of nodes in the graph: variable, mapping, and sum nodes. Let U , M_a , V , M_b , and Y be five node sets that include the nodes below letters “ U ,” “ M_a ,” “ V ,” “ M_b ,” and “ Y ” in Fig. 2. The variable node in U corresponds to an information bit. The variable node in V corresponds to a symbol in $\text{GF}(2^s)$. The mapping node in M_a or M_b denotes a mapping relation between a $\text{GF}(2^s)$ symbol and s bits. The sum node in Y , associated with a received symbol, denotes a superposition of the transmitted symbols from K users. Note that the sum node connects the remaining $K - 1$ user’s factor graphs. Edges connecting variable nodes in V and mapping nodes in M_b

are labeled by elements of spreading vector $s^{(k)}$. During encoding and decoding, the message should multiply the labeled element or its inverse when passing across one of these edges.

B. Iterative Decoding

The iterative decoding is performed on the factor graph in Fig. 2 and is accomplished by efficient local decoding at all the nodes and interactions. The input and output of local decoding at each node is denoted by a log-likelihood ratio (LLR). Since the decoding of each user is performed in parallel and is the same, we only give decoding algorithm for user k .

A single decoding iteration includes the local decoding at the sum node in Y , deinterleaving, and the FF-DES in Fig. 2. For the local decoding at the sum node in Y , we employ the low-complexity elementary signal estimation (ESE) algorithm given in [3]–[5]. For the FF-DES, we give a maximum a posteriori probability (MAP) decoding algorithm. After a number of iterations, a hard decision is performed to recover the information vector.

1) *Sum Node Decoding (ESE)*: Let $L^a(x_t^{(i)})$, $1 \leq i \leq K, i \neq k$, denote a priori LLR of $x_t^{(i)}$ in (1) to the t -th, $1 \leq t \leq sNL$, sum node in Y . By regarding $\sum_{i=1, i \neq k}^K \sqrt{\frac{E_b}{L}} x_t^{(i)}$ as a Gaussian variable, this sum node performs a local decoding and outputs an extrinsic LLR of $x_t^{(k)}$ as [3]–[5]

$$\begin{aligned} L^e(x_t^{(k)}) &= \log \frac{\Pr(x_t^{(k)} = +1 | y_t)}{\Pr(x_t^{(k)} = -1 | y_t)} \\ &= \frac{2 \sqrt{\frac{E_b}{L}} \left(y_t - \sqrt{\frac{E_b}{L}} \sum_{i=1, i \neq k}^K \tanh\left(\frac{L^a(x_t^{(i)})}{2}\right) \right)}{\frac{E_b}{L} \sum_{i=1, i \neq k}^K \left(1 - \left(\tanh\left(\frac{L^a(x_t^{(i)})}{2}\right) \right)^2 \right) + \frac{N_0}{2}} \end{aligned} \quad (2)$$

which will be deinterleaved as a priori LLR for the FF-DES.

2) *FF-DES*: After deinterleaving, we obtain a priori LLR $L^a(c_t^{(k)})$, $1 \leq t \leq sNL$, for each chip of user k . The FF-DES will calculate an extrinsic LLR $L^e(c_t^{(k)})$ based on the priori LLRs $L^a(c_t^{(k)})$, $1 \leq t \leq sNL$, by the local decoding at the nodes in $M_b \rightarrow V \rightarrow M_b$, subsequently.

Since the decoding operation for each chip is the same, to simplify our description, we only introduce the calculation of extrinsic LLR $L^e(c_{(\ell-1)s+n}^{(k)})$, $1 \leq \ell \leq L, 1 \leq n \leq s$, performed on the subgraph associated with the first variable node in V of Fig. 2.

Let $(L^a(c_{(i-1)s+1}^{(k)}), \dots, L^a(c_{is}^{(k)}))$ denote the s chip-LLR inputs to the i -th, $1 \leq i \leq L$, mapping node in M_b and $\mathbf{y}'_i = (y'_{(i-1)s+1}, \dots, y'_{is})$ denote the associated received symbols ($\mathbf{y}' = (y'_1, \dots, y'_{sNL})$ is the deinterleaved form of \mathbf{y}). This mapping node performs a local decoding to transform

chip LLRs to field symbol LLR vector $\mathbf{L}^a(\gamma_i^{(k)}) = (L_0^a(\gamma_i^{(k)}), L_1^a(\gamma_i^{(k)}), \dots, L_{\alpha^{2^s-2}}^a(\gamma_i^{(k)}))$ of $\gamma_i^{(k)}$ as

$$\begin{aligned}
L_\lambda^a(\gamma_i^{(k)}) &= \log \frac{\Pr(\gamma_i^{(k)} = \lambda | \mathbf{y}'_i)}{\Pr(\gamma_i^{(k)} = 0 | \mathbf{y}'_i)} \\
&= \log \frac{\prod_{m=1}^s \Pr(c_{(i-1)s+m}^{(k)} = \Gamma_m^{-1}(\lambda) | \mathbf{y}'_{(i-1)s+m})}{\prod_{m=1}^s \Pr(c_{(i-1)s+m}^{(k)} = \Gamma_m^{-1}(0) | \mathbf{y}'_{(i-1)s+m})} \\
&= \log \frac{\prod_{m=1}^s \frac{\Pr(c_{(i-1)s+m}^{(k)} = \Gamma_m^{-1}(\lambda) | \mathbf{y}'_{(i-1)s+m})}{\Pr(c_{(i-1)s+m}^{(k)} = -1 | \mathbf{y}'_{(i-1)s+m})}}{\prod_{m=1}^s \frac{\Pr(c_{(i-1)s+m}^{(k)} = \Gamma_m^{-1}(0) | \mathbf{y}'_{(i-1)s+m})}{\Pr(c_{(i-1)s+m}^{(k)} = -1 | \mathbf{y}'_{(i-1)s+m})}} \\
&= \log \frac{\prod_{m=1}^s \left(\frac{\Pr(c_{(i-1)s+m}^{(k)} = +1 | \mathbf{y}'_{(i-1)s+m})}{\Pr(c_{(i-1)s+m}^{(k)} = -1 | \mathbf{y}'_{(i-1)s+m})} \right)^{\frac{(1+\Gamma_m^{-1}(\lambda))}{2}}}{\prod_{m=1}^s \left(\frac{\Pr(c_{(i-1)s+m}^{(k)} = +1 | \mathbf{y}'_{(i-1)s+m})}{\Pr(c_{(i-1)s+m}^{(k)} = -1 | \mathbf{y}'_{(i-1)s+m})} \right)^{\frac{(1+\Gamma_m^{-1}(0))}{2}}} \\
&= \sum_{m=1}^s \frac{\Gamma_m^{-1}(\lambda) - \Gamma_m^{-1}(0)}{2} L^a(c_{(i-1)s+m}^{(k)}), \quad \lambda = 0, 1, \dots, \alpha^{2^s-2} \tag{3}
\end{aligned}$$

where $\Gamma_m^{-1}(\lambda)$ takes the m -th bit of the demapped vector $\Gamma^{-1}(\lambda)$. Here we use a posteriori probability of zero element 0 as the denominator in a field symbol LLR.

Let $\mathbf{y}'_{\neq \ell} = (\mathbf{y}'_1, \dots, \mathbf{y}'_{l-1}, \mathbf{y}'_{l+1}, \dots, \mathbf{y}'_L)$ denote the joint vector of $\mathbf{y}'_i, i = 1, \dots, L, i \neq \ell$. Similarly, we have denotation $\mathbf{s}_{\neq \ell}^{(k)} = (s_1^{(k)}, \dots, s_{\ell-1}^{(k)}, s_{\ell+1}^{(k)}, \dots, s_L^{(k)})$. Based on the $L-1$ field symbol LLR vectors $\mathbf{L}^a(\gamma_i^{(k)}), 1 \leq i \leq L, i \neq \ell$, the first variable node in V performs a local decoding to calculate the extrinsic LLR vector $\mathbf{L}^e(\gamma_\ell^{(k)}) = (L_0^e(\gamma_\ell^{(k)}), L_1^e(\gamma_\ell^{(k)}), \dots, L_{\alpha^{2^s-2}}^e(\gamma_\ell^{(k)}))$ of $\gamma_\ell^{(k)}$ as

$$\begin{aligned}
L_\lambda^e(\gamma_\ell^{(k)}) &= \log \frac{\Pr(\gamma_\ell^{(k)} = \lambda | \mathbf{y}'_{\neq \ell})}{\Pr(\gamma_\ell^{(k)} = 0 | \mathbf{y}'_{\neq \ell})} \\
&= \log \frac{\Pr(\beta_1^{(k)} = \lambda (s_\ell^{(k)})^{-1} | \mathbf{y}'_{\neq \ell})}{\Pr(\beta_1^{(k)} = 0 | \mathbf{y}'_{\neq \ell})} \\
&= \log \frac{\Pr(\beta_1^{(k)} \mathbf{s}_{\neq \ell}^{(k)} = \lambda (s_\ell^{(k)})^{-1} \mathbf{s}_{\neq \ell}^{(k)} | \mathbf{y}'_{\neq \ell})}{\Pr(\beta_1^{(k)} \mathbf{s}_{\neq \ell}^{(k)} = \mathbf{0}_{L-1} | \mathbf{y}'_{\neq \ell})} \\
&= \log \frac{\prod_{i=1, i \neq \ell}^L \Pr(\gamma_i^{(k)} = \lambda (s_\ell^{(k)})^{-1} s_i^{(k)} | \mathbf{y}'_i)}{\prod_{i=1, i \neq \ell}^L \Pr(\gamma_i^{(k)} = 0 | \mathbf{y}'_i)} \\
&= \sum_{i=1, i \neq \ell}^L L_{\lambda (s_\ell^{(k)})^{-1} s_i^{(k)}}^a(\gamma_i^{(k)}), \quad \lambda = 0, 1, \dots, \alpha^{2^s-2} \tag{4}
\end{aligned}$$

where $\mathbf{0}_{L-1} = (0, \dots, 0)$ is a length- $(L-1)$ zero vector and $(s_\ell^{(k)})^{-1}$ is the inverse of $s_\ell^{(k)}$ in $\text{GF}(2^s)$.

The ℓ -th, $1 \leq \ell \leq L$, mapping node in M_b transforms the extrinsic symbol LLR vector $L^e(\gamma_\ell^{(k)})$ to extrinsic chip LLRs of $c_{(\ell-1)s+n}^{(k)}$ as

$$\begin{aligned}
L^e(c_{(\ell-1)s+n}^{(k)}) &= \log \frac{\Pr(c_{(\ell-1)s+n}^{(k)} = +1 | \mathbf{y}'_{\chi\ell})}{\Pr(c_{(\ell-1)s+n}^{(k)} = -1 | \mathbf{y}'_{\chi\ell})} \\
&= \log \frac{\sum_{\lambda \in \text{GF}(2^s), \Gamma_n^{-1}(\lambda) = +1} \Pr(\gamma_\ell^{(k)} = \lambda | \mathbf{y}'_{\chi\ell})}{\sum_{\lambda \in \text{GF}(2^s), \Gamma_n^{-1}(\lambda) = -1} \Pr(\gamma_\ell^{(k)} = \lambda | \mathbf{y}'_{\chi\ell})} \\
&= \log \frac{\sum_{\lambda \in \text{GF}(2^s)} \frac{1 + \Gamma_n^{-1}(\lambda)}{2} \frac{\Pr(\gamma_\ell^{(k)} = \lambda | \mathbf{y}'_{\chi\ell})}{\Pr(\gamma_\ell^{(k)} = 0 | \mathbf{y}'_{\chi\ell})}}{\sum_{\lambda \in \text{GF}(2^s)} \frac{1 - \Gamma_n^{-1}(\lambda)}{2} \frac{\Pr(\gamma_\ell^{(k)} = \lambda | \mathbf{y}'_{\chi\ell})}{\Pr(\gamma_\ell^{(k)} = 0 | \mathbf{y}'_{\chi\ell})}} \\
&= \log \frac{\sum_{\lambda \in \text{GF}(2^s)} (1 + \Gamma_n^{-1}(\lambda)) e^{L_\lambda^e(\gamma_\ell^{(k)})}}{\sum_{\lambda \in \text{GF}(2^s)} (1 - \Gamma_n^{-1}(\lambda)) e^{L_\lambda^e(\gamma_\ell^{(k)})}}, \quad n = 1, \dots, s. \tag{5}
\end{aligned}$$

These extrinsic chip LLRs will be interleaved to update the priori LLRs of the sum node decoding in (2).

3) *Hard Decision*: The hard decision is performed on the output from the mapping node in M_a to the variable node in U . Using a similar principle as in (4), the first variable node in V calculates a total posteriori LLR vector $L(\beta_1^{(k)}) = (L_0(\beta_1^{(k)}), L_1(\beta_1^{(k)}), \dots, L_{\alpha^{2^s-2}}(\beta_1^{(k)}))$ of $\beta_1^{(k)}$ as

$$L_\lambda(\beta_1^{(k)}) = \sum_{i=1}^L L_{\lambda s_i^{(k)}}^a(\gamma_i^{(k)}), \quad \lambda = 0, 1, \dots, \alpha^{2^s-2}. \tag{6}$$

The first mapping node in M_a transforms this field symbol LLR vector to s bit LLRs using a similar principle as in (5)

$$L(u_n) = \log \frac{\sum_{\lambda \in \text{GF}(2^s)} (1 + \Gamma_n^{-1}(\lambda)) e^{L_\lambda(\beta_1^{(k)})}}{\sum_{\lambda \in \text{GF}(2^s)} (1 - \Gamma_n^{-1}(\lambda)) e^{L_\lambda(\beta_1^{(k)})}}, \quad n = 1, \dots, s \tag{7}$$

for bit decision. Note that the mapping node in M_a does not provide any message to the variable node in V during the iterative decoding. Here we give a bit decision algorithm, in which the hard decision is performed on the LLRs of information bits in (7). The hard decision can also be performed on the field symbol LLR in (6) to obtain an estimation of $\beta_1^{(k)}$.

IV. ANALYSIS OF EXIT FUNCTION OF FF-DES

To show the performance gain of joint spreading quantitatively, we analyze the EXIT function of the FF-DES. In Section IV-A, we give an approximate EXIT function and show that this EXIT function asymptotically approaches a line. In Section IV-B, we derive the asymptotic slope of the EXIT function.

A. Approximate EXIT Function

The EXIT function describes a relation between the priori input and the extrinsic output of a decoding. Both the input and the output of the decoding are measured by mutual information or LLR mean value based on the Gaussian approximation [7]–[10]. In this section, we give an approximate EXIT function of the FF-DES using the measure of LLR mean value.

The EXIT function of FF-DES describes the relation between the mean value of a priori chip LLR and that of the extrinsic chip LLR. Generally, this EXIT function is determined by the realizations of a specific chip, mapping Γ , and spreading vector $s^{(k)}$. Here we consider random chip, random mapping Γ , and random spreading vector $s^{(k)}$, all of which are uniformly generated from all their possible realizations. We derive an expected EXIT function that is an average for all the possible chip, mapping, and spreading vector realizations.

Since as stated in Section III, the decoding operation for each chip of each user is the same, we omit superscript (k) to consider the chip $c_{(\ell-1)s+n}$, $1 \leq \ell \leq L$, $1 \leq n \leq s$, in our analysis. The EXIT function is the function between $E[c_{(\ell-1)s+n}L^e(c_{(\ell-1)s+n})]$ and $E[c_{(i-1)s+m}L^a(c_{(i-1)s+m})]$, $i \neq \ell$, $1 \leq m \leq s$, where $E[\cdot]$ takes the expectation of a random variable.

Combining (3), (4), and (5) in the FF-DES, we write $L^e(c_{(\ell-1)s+n})$ as a function of $L^a(c_{(i-1)s+m})$, $i \neq \ell$, $1 \leq m \leq s$,

$$\begin{aligned} L^e(c_{(\ell-1)s+n}) &= \log \frac{\sum_{\lambda \in \text{GF}(2^s)} (1 + \Gamma_n^{-1}(\lambda)) e^{\sum_{i=1, i \neq \ell}^L \sum_{m=1}^s \frac{\Gamma_m^{-1}(\lambda(s_\ell)^{-1} s_i) - \Gamma_m^{-1}(0)}{2} L^a(c_{(i-1)s+m})}}{\sum_{\lambda \in \text{GF}(2^s)} (1 - \Gamma_n^{-1}(\lambda)) e^{\sum_{i=1, i \neq \ell}^L \sum_{m=1}^s \frac{\Gamma_m^{-1}(\lambda(s_\ell)^{-1} s_i) - \Gamma_m^{-1}(0)}{2} L^a(c_{(i-1)s+m})}} \\ &= \log \frac{\sum_{\lambda \in \text{GF}(2^s)} (1 + \Gamma_n^{-1}(\lambda)) e^{\rho(\lambda)}}{\sum_{\lambda \in \text{GF}(2^s)} (1 - \Gamma_n^{-1}(\lambda)) e^{\rho(\lambda)}} \end{aligned} \quad (8)$$

where $\rho(\lambda) \triangleq \frac{1}{2} \sum_{i=1, i \neq \ell}^L \sum_{m=1}^s \Gamma_m^{-1}(\lambda(s_\ell)^{-1} s_i) L^a(c_{(i-1)s+m})$.

By the Gaussian approximation [7] [8], $c_{(i-1)s+m}L^a(c_{(i-1)s+m}) \sim \mathcal{N}(m_a, 2m_a)$, $1 \leq i \leq L$, $1 \leq m \leq s$, i.i.d., and $c_{(\ell-1)s+n}L^e(c_{(\ell-1)s+n}) \sim \mathcal{N}(m_e, 2m_e)$, where $\mathcal{N}(\mu, \sigma^2)$ denotes the Gaussian

distribution with mean μ and variance σ^2 . Based on (8), the EXIT function becomes

$$\begin{aligned}
m_e &= E[c_{(\ell-1)s+n} L^e(c_{(\ell-1)s+n})] \\
&= E[c_{(\ell-1)s+n} \log \frac{\sum_{\lambda \in \text{GF}(2^s)} (1 + \Gamma_n^{-1}(\lambda)) e^{\rho(\lambda)}}{\sum_{\lambda \in \text{GF}(2^s)} (1 - \Gamma_n^{-1}(\lambda)) e^{\rho(\lambda)}}] \\
&= E[\log \frac{\sum_{\lambda \in \text{GF}(2^s)} (1 + c_{(\ell-1)s+n} \Gamma_n^{-1}(\lambda)) e^{\rho(\lambda)}}{\sum_{\lambda \in \text{GF}(2^s)} (1 - c_{(\ell-1)s+n} \Gamma_n^{-1}(\lambda)) e^{\rho(\lambda)}}] \\
&= E[\log \frac{(1 + c_{(\ell-1)s+n} \Gamma_n^{-1}(\gamma_\ell)) e^{\rho(\gamma_\ell)} + \sum_{\lambda \in \text{GF}(2^s), \lambda \neq \gamma_\ell} (1 + c_{(\ell-1)s+n} \Gamma_n^{-1}(\lambda)) e^{\rho(\lambda)}}{(1 - c_{(\ell-1)s+n} \Gamma_n^{-1}(\gamma_\ell)) e^{\rho(\gamma_\ell)} + \sum_{\lambda \in \text{GF}(2^s), \lambda \neq \gamma_\ell} (1 - c_{(\ell-1)s+n} \Gamma_n^{-1}(\lambda)) e^{\rho(\lambda)}}] \\
&= E[\log \frac{2e^{\rho(\gamma_\ell)} + \sum_{\lambda \in \text{GF}(2^s), \lambda \neq \gamma_\ell} (1 + c_{(\ell-1)s+n} \Gamma_n^{-1}(\lambda)) e^{\rho(\lambda)}}{\sum_{\lambda \in \text{GF}(2^s), \lambda \neq \gamma_\ell} (1 - c_{(\ell-1)s+n} \Gamma_n^{-1}(\lambda)) e^{\rho(\lambda)}}] \tag{9} \\
&= E[2\rho(\gamma_\ell)] + E[\log \frac{1 + \frac{1}{2} \sum_{\lambda \in \text{GF}(2^s), \lambda \neq \gamma_\ell} (1 + c_{(\ell-1)s+n} \Gamma_n^{-1}(\lambda)) e^{\rho(\lambda) - \rho(\gamma_\ell)}}{\frac{1}{2} \sum_{\lambda \in \text{GF}(2^s), \lambda \neq \gamma_\ell} (1 - c_{(\ell-1)s+n} \Gamma_n^{-1}(\lambda)) e^{\rho(\lambda) + \rho(\gamma_\ell)}}] \\
&= s(L-1)m_a - E[\log(\sum_{\lambda \in \lambda^-} e^{\rho(\gamma_\ell) + \rho(\lambda)})] + E[\log(1 + \sum_{\lambda \in \lambda^+} e^{-\rho(\gamma_\ell) - \rho(\lambda)})]. \tag{10}
\end{aligned}$$

Eq. (9) is from the fact $\Gamma_n^{-1}(\gamma_\ell) = c_{(\ell-1)s+n}$ since γ_ℓ is the correct symbol. In (10), the first term is from $\rho(\gamma_\ell) = \frac{1}{2} \sum_{i=1, i \neq \ell}^L \sum_{m=1}^s c_{(i-1)s+m} L^a(c_{(i-1)s+m})$ due to $\Gamma_m^{-1}(\gamma_\ell(s_\ell)^{-1} s_i) = c_{(i-1)s+m}$. In the second and third terms, $\lambda^- \triangleq \{\lambda | \lambda \in \text{GF}(2^s), \Gamma_n^{-1}(\lambda) = -c_{(\ell-1)s+n}\}$ and $\lambda^+ \triangleq \{\lambda | \lambda \in \text{GF}(2^s), \lambda \neq \gamma_\ell, \Gamma_n^{-1}(\lambda) = c_{(\ell-1)s+n}\}$. It holds that $|\lambda^-| = 2^{s-1}$, $|\lambda^+| = 2^{s-1} - 1$, where $|\cdot|$ takes the cardinality of a set.

Now we give an approximation for the EXIT function in (10). For $\lambda \in \lambda^-$, we have

$$\begin{aligned}
\rho(\gamma_\ell) + \rho(\lambda) &= \frac{1}{2} \sum_{i=1, i \neq \ell}^L \sum_{m=1}^s (c_{(i-1)s+m} + \Gamma_m^{-1}(\lambda(s_\ell)^{-1} s_i)) L^a(c_{(i-1)s+m}) \\
&= \sum_{i=1, i \neq \ell}^L \sum_{m=1}^s \frac{(1 + c_{(i-1)s+m} \Gamma_m^{-1}(\lambda(s_\ell)^{-1} s_i))}{2} c_{(i-1)s+m} L^a(c_{(i-1)s+m}). \tag{11}
\end{aligned}$$

Similarly, for $\lambda \in \lambda^+$, we have

$$\rho(\gamma_\ell) - \rho(\lambda) = \sum_{i=1, i \neq \ell}^L \sum_{m=1}^s \frac{(1 - c_{(i-1)s+m} \Gamma_m^{-1}(\lambda(s_\ell)^{-1} s_i))}{2} c_{(i-1)s+m} L^a(c_{(i-1)s+m}). \tag{12}$$

Vector $(c_{(i-1)s+1} \Gamma_1^{-1}(\lambda(s_\ell)^{-1} s_i), \dots, c_{is} \Gamma_s^{-1}(\lambda(s_\ell)^{-1} s_i))$ in (11) and (12) is a bit-wise correlation between the binary vectors for the correct symbol and an error symbol. Due to random chip $c_{(i-1)s+m}$, random mapping Γ , and random spreading element s_i , this bit-wise correlation vector is approximately uniformly distributed on the set that includes all the binary vector in \mathcal{X}^s except all-one vector $\mathbf{1}_s = (1, \dots, 1)$. Let set Ω_s^- include all the binary- $\{0, 1\}$ vectors of length s except $\mathbf{1}_s$, and Ω_s^+ include all the binary- $\{0, 1\}$ vectors of length s except $\mathbf{0}_s$. Let $\mathcal{U}(\Omega)$

denote the uniform distribution on set Ω . We have the following approximation of the EXIT function (10)

$$m_e \approx s(L-1)m_a - E[\log(\sum_{j=1}^{2^{s-1}} e^{\sum_{i=1}^{L-1} \mathbf{r}_{j,i} \mathbf{h}_i^T})] + E[\log(1 + \sum_{j=1}^{2^{s-1}-1} e^{-\sum_{i=1}^{L-1} \mathbf{r}'_{j,i} \mathbf{h}_i^T})] \triangleq \varphi(m_a) \quad (13)$$

where $\mathbf{r}_{j,i}, j = 1, \dots, 2^{s-1}, i = 1, \dots, L-1$, are i.i.d. with $\mathbf{r}_{j,i} \sim \mathcal{U}(\Omega_s^-)$. Vectors $\mathbf{r}'_{j,i}, j = 1, \dots, 2^{s-1}-1, i = 1, \dots, L-1$, are i.i.d. with $\mathbf{r}'_{j,i} \sim \mathcal{U}(\Omega_s^+)$. Elements $h_{i,m}, i = 1, \dots, L, m = 1, \dots, s$, in $\mathbf{h}_i, i = 1, \dots, L$, are all i.i.d. with $h_{i,m} \sim \mathcal{N}(m_a, 2m_a)$.

To see the accuracy of the approximation in (13), Figs. 3 and 4 illustrate the EXIT function in (10) and $\varphi(m_a)$ in (13) for $L = 8, 16$ and $s = 1, 2, 4, 6$ by Monte Carlo simulations. We see that $\varphi(m_a)$ is in fact a tight upper bound of the EXIT function. The ratio between $\varphi(m_a)$ and the EXIT function is less than 1.06 for $m_a \leq 10$ in both figures. Based on this fact, in the rest analysis of this paper, we employ approximate EXIT function $\varphi(m_a)$ of the FF-DES.

Moreover, we have the following observation on the approximate EXIT function. There exists a cutoff point m_0 usually less than 1. For $m_a \geq m_0$, every curve of the approximate EXIT function in Figs. 3 and 4 asymptotically approaches a line. The asymptotic slope of the approximate EXIT function increases as s increases. This means that by joint spreading for s information bits, an SINR gain is obtained with respect to that of $s = 1$. This SINR gain will be enhanced as length s increases. Furthermore, by comparing Fig. 3 and Fig. 4 we can see that given s , the asymptotic slope of the approximate EXIT function for $L = 16$ is larger than that for $L = 8$. This is due to that as spreading length L increases, the advantage of joint spreading is enlarged.

Remark 1: Although we have focused on the asymptotic slope of the EXIT function of the FF-DES when m_a is large above, the EXIT function at m_a near 0 is also noteworthy. If the number of users K is large, due to a large multi-user interference, at the beginning of decoding iteration the extrinsic output of the ESE is always very small. This requires the EXIT function of the FF-DES to be sufficiently large at m_a near 0, or else the iterative decoding would fail at the beginning of iteration. As revealed in [11] and [12], conventional spreading scheme is widely used in the MAC since it can provide a large EXIT function at m_a near 0. We see that in Figs. 3 and 4, the finite field spreading can provide a similar EXIT function as that of the conventional spreading scheme ($s = 1$) at $m_a < m_0$, and can also work in the environment of large multi-user interference.

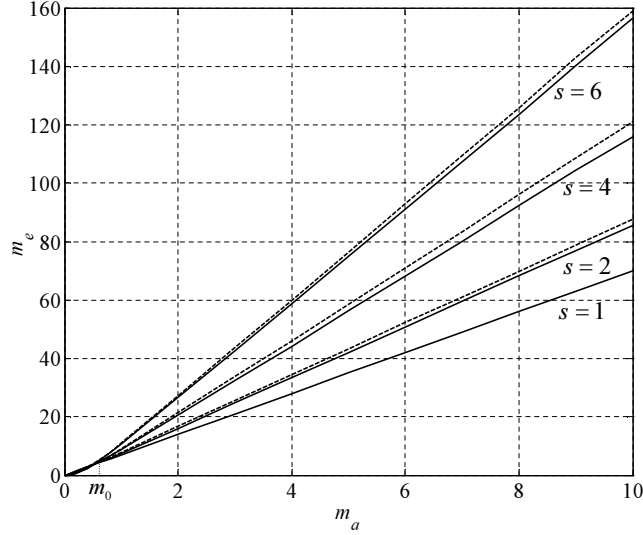


Fig. 3. EXIT functions (solid lines) and their approximations of $\varphi(m_a)$ (dashed lines) of the FF-DES for $L = 8$ and $s = 1, 2, 4, 6$.

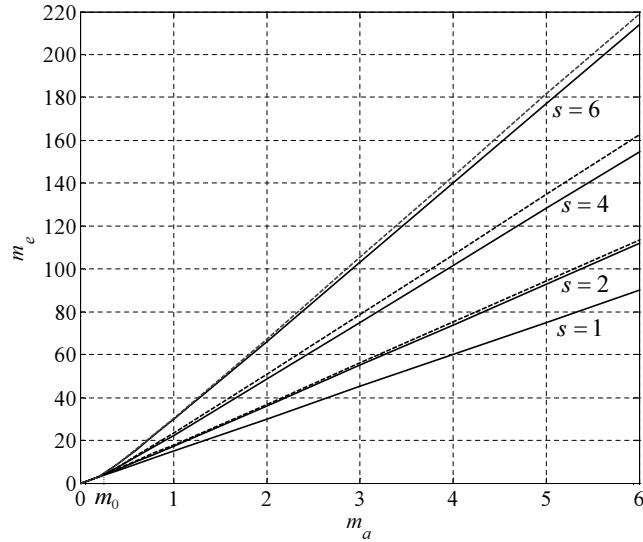


Fig. 4. EXIT functions (solid lines) and their approximations of $\varphi(m_a)$ (dashed lines) of the FF-DES for $L = 16$ and $s = 1, 2, 4, 6$.

B. Asymptotic Slope

Section IV-A has shown that when m_a is larger than cutoff point m_0 , the approximate EXIT function of FF-DES asymptotically approaches a line. In this section, we analyze this slope by deriving the asymptotic differential of $\varphi(m_a)$ in (13).

Theorem 1: Let $g(s, L)$ be a function of s and L . Let $m_0 \geq 0$ be a constant. Suppose that

$\varphi(m_a) = \varphi(m_0) + g(s, L)(m_a - m_0)$ holds for $m_a \geq m_0$, we have

$$g(s, L) = L - 1 + \frac{1}{(2^s - 1)^{(L-1)2^{s-1}}} \sum_{k=1}^{(s-1)(L-1)} \left(\sum_{(n_1, \dots, n_{L-1}) \in \theta(k-1)} \prod_{i=1}^{L-1} \binom{s}{n_i} \right)^{2^{s-1}} \quad (14)$$

where $\theta(k-1) \triangleq \{n_1, \dots, n_{L-1} \mid \sum_{i=1}^{L-1} n_i \leq k-1, 0 \leq n_i \leq s-1, n_i \in \mathbb{Z}\}$ with integer set \mathbb{Z} . \square

To prove Theorem 1, we first prove the following lemma.

Lemma 1: Let $a \geq 1$ be a constant. Let $\widehat{\mathbf{r}}_j = [\widehat{r}_{j,1}, \dots, \widehat{r}_{j,m}]$, $\widehat{r}_{j,i} \in \{-1, 0, 1\}$, $j = 1, \dots, n$, be i.i.d. random vectors with $w(\widehat{\mathbf{r}}_j) \triangleq \sum_{i=1}^m \widehat{r}_{j,i} \leq 0$, and $w^+(\widehat{\mathbf{r}}_j) \triangleq \sum_{i=1}^m |\widehat{r}_{j,i}| > 0$ for all j . Let $\widehat{\mathbf{h}}$ be a length- m vector whose elements are i.i.d. with Gaussian distribution $\mathcal{N}(\mu, 2\mu)$, $\mu > 0$. It holds that

$$\lim_{\mu \rightarrow +\infty} \frac{E[\log(a + \sum_{j=1}^n e^{\widehat{\mathbf{r}}_j \widehat{\mathbf{h}}^T})]}{\mu} = 0. \quad (15)$$

\square

Proof: We first have

$$\begin{aligned} 0 &\leq E[\log(a + \sum_{j=1}^n e^{\widehat{\mathbf{r}}_j \widehat{\mathbf{h}}^T})] \leq E[\log(a + \sum_{j=1}^n e^{\widehat{\mathbf{r}}_j \widehat{\mathbf{h}}^T - w(\widehat{\mathbf{r}}_j)\mu})] \\ &\leq E[\log((n+1) \max\{a, e^{\widehat{\mathbf{r}}_1 \widehat{\mathbf{h}}^T - w(\widehat{\mathbf{r}}_1)\mu}, \dots, e^{\widehat{\mathbf{r}}_n \widehat{\mathbf{h}}^T - w(\widehat{\mathbf{r}}_n)\mu}\})] \\ &\leq \log(n+1) + E[\log(a + \sum_{j=1}^n |\widehat{\mathbf{r}}_j \widehat{\mathbf{h}}^T - w(\widehat{\mathbf{r}}_j)\mu|)] \\ &= \log(a(n+1)) + n \sum_{k=1}^m E[|\widehat{\mathbf{r}}_1 \widehat{\mathbf{h}}^T - w(\widehat{\mathbf{r}}_1)\mu| \mid w^+(\widehat{\mathbf{r}}_1) = k] \Pr(w^+(\widehat{\mathbf{r}}_1) = k) \\ &= \log(a(n+1)) + 2n \sum_{k=1}^m \sqrt{\frac{k\mu}{\pi}} \Pr(w^+(\widehat{\mathbf{r}}_1) = k) \\ &\leq \log(a(n+1)) + 2n \sqrt{\frac{m\mu}{\pi}} \end{aligned} \quad (16)$$

where (16) is due to that under the condition $w^+(\widehat{\mathbf{r}}_1) = k$, $(\widehat{\mathbf{r}}_1 \widehat{\mathbf{h}}^T - w(\widehat{\mathbf{r}}_1)\mu) \sim \mathcal{N}(0, 2k\mu)$ holds for each realization of $\widehat{\mathbf{r}}_1$. Thus,

$$0 \leq \lim_{\mu \rightarrow +\infty} \frac{E[\log(a + \sum_{j=1}^n e^{\widehat{\mathbf{r}}_j \widehat{\mathbf{h}}^T})]}{\mu} \leq \lim_{\mu \rightarrow +\infty} \frac{\log(a(n+1)) + 2n \sqrt{\frac{m\mu}{\pi}}}{\mu} = 0.$$

The lemma is proved.

Proof of Theorem 1: Let $J_{\max} \triangleq \{j^* \mid j^* = \arg \max_j \{\sum_{i=1}^{L-1} w(\mathbf{r}_{j,i})\}\}$ be the set of subscripts that maximize the Hamming weight of joint vector $(\mathbf{r}_{j,1}, \dots, \mathbf{r}_{j,L-1})$ in (13). Given an element of $j^* \in J_{\max}$, we have set $J^* \triangleq \{j \mid \mathbf{r}_{j,i} = \mathbf{r}_{j^*,i}, i = 1, \dots, L-1\} \subseteq J_{\max}$.

Since $\varphi(m_a) = \varphi(m_0) + g(s, L)(m_a - m_0)$ holds as $m_a \rightarrow +\infty$ by assumption, using (13) we have

$$\begin{aligned} g(s, L) &= \lim_{m_a \rightarrow +\infty} \frac{\varphi(m_a) - \varphi(m_0)}{m_a - m_0} = \lim_{m_a \rightarrow +\infty} \frac{\varphi(m_a)}{m_a} \\ &= s(L-1) - \lim_{m_a \rightarrow +\infty} \frac{E[\log(\sum_{j=1}^{2^{s-1}} e^{\sum_{i=1}^{L-1} \mathbf{r}_{j,i} \mathbf{h}_i^T})]}{m_a} + \lim_{m_a \rightarrow +\infty} \frac{E[\log(1 + \sum_{j=1}^{2^{s-1}-1} e^{-\sum_{i=1}^{L-1} \mathbf{r}_{j,i} \mathbf{h}_i^T})]}{m_a} \\ &= s(L-1) - \lim_{m_a \rightarrow +\infty} \frac{E[\log(\sum_{j=1}^{2^{s-1}} e^{\sum_{i=1}^{L-1} \mathbf{r}_{j,i} \mathbf{h}_i^T})]}{m_a} \end{aligned} \quad (17)$$

$$\begin{aligned} &= s(L-1) - \lim_{m_a \rightarrow +\infty} \frac{E[\sum_{i=1}^{L-1} \mathbf{r}_{j^*,i} \mathbf{h}_i^T]}{m_a} - \lim_{m_a \rightarrow +\infty} \frac{E[\log(|j^*| + \sum_{j=1, j \neq j^*}^{2^{s-1}} e^{-\sum_{i=1}^{L-1} (\mathbf{r}_{j^*,i} - \mathbf{r}_{j,i}) \mathbf{h}_i^T})]}{m_a} \\ &= s(L-1) - E\left[\sum_{i=1}^{L-1} w(\mathbf{r}_{j^*,i})\right] \end{aligned} \quad (18)$$

$$\begin{aligned} &= s(L-1) - \sum_{k=1}^{(s-1)(L-1)} k \Pr\left(\sum_{i=1}^{L-1} w(\mathbf{r}_{j^*,i}) = k\right) \\ &= s(L-1) - \sum_{k=1}^{(s-1)(L-1)} k \left(\Pr\left(\sum_{i=1}^{L-1} w(\mathbf{r}_{j^*,i}) \leq k\right) - \Pr\left(\sum_{i=1}^{L-1} w(\mathbf{r}_{j^*,i}) \leq k-1\right) \right) \\ &= s(L-1) - (s-1)(L-1) \Pr\left(\sum_{i=1}^{L-1} w(\mathbf{r}_{j^*,i}) \leq (s-1)(L-1)\right) + \sum_{k=1}^{(s-1)(L-1)} \Pr\left(\sum_{i=1}^{L-1} w(\mathbf{r}_{j^*,i}) \leq k-1\right) \\ &= L-1 + \sum_{k=1}^{(s-1)(L-1)} \Pr\left(\sum_{i=1}^{L-1} w(\mathbf{r}_{1,i}) \leq k-1, \dots, \sum_{i=1}^{L-1} w(\mathbf{r}_{2^{s-1},i}) \leq k-1\right) \\ &= L-1 + \sum_{k=1}^{(s-1)(L-1)} \left(\Pr\left(\sum_{i=1}^{L-1} w(\mathbf{r}_{1,i}) \leq k-1\right) \right)^{2^{s-1}} \end{aligned} \quad (19)$$

$$= L-1 + \frac{1}{(2^s - 1)^{(L-1)2^{s-1}}} \sum_{k=1}^{(s-1)(L-1)} \left(\sum_{(n_1, \dots, n_{L-1}) \in \theta(k-1)} \prod_{i=1}^{L-1} \binom{s}{n_i} \right)^{2^{s-1}}. \quad (20)$$

Eq. (17) is from Lemma 1. Eq. (18) is due to that elements of \mathbf{h}_i are i.i.d. with distribution $\mathcal{N}(m_a, 2m_a)$ and Lemma 1. Eq. (19) is due to that $\sum_{i=1}^{L-1} w(\mathbf{r}_{j,i})$, $j = 1, \dots, 2^{s-1}$, are i.i.d.. Eq. (20) is due to that $\mathbf{r}_{1,i}$, $i = 1, \dots, L-1$, are i.i.d. with $\mathbf{r}_{1,i} \sim \mathcal{U}(\Omega_s^-)$. The theorem is proved. \square

For $s = 1$, $g(1, L) = L-1$ is the slope of the EXIT function of the DES for the conventional spreading scheme of IDMA [3]–[5]. The last term in (20) is the slope gain from the joint spreading.

V. SLOPE OF BER

In this section, we show that the asymptotic slope of approximate EXIT function analyzed in Section IV-B in fact is the absolute slope of BER curve at the low BER region. We

verify our analysis by BER Monte Carlo simulations for practical finite field multiple-access systems.

Let $\phi(m_a, \frac{E_b}{N_0})$ be the EXIT function of the ESE (Appendix A). The mean of extrinsic LLR converges to infinity as the number of iteration increases if and only if $\phi(x, \frac{E_b}{N_0}) > \varphi^{-1}(x)$ holds for $x \geq 0$ [7]–[10], where $\varphi^{-1}(\cdot)$ is the inverse function of $\varphi(\cdot)$ in (13). Since $\phi(x, \frac{E_b}{N_0}) \leq 4\frac{E_b}{LN_0}$ (Lemma 2 in Appendix A) and $\lim_{x \rightarrow +\infty} \varphi^{-1}(x) = +\infty$, to converge to infinite mean of LLR, $\frac{E_b}{N_0}$ should approach infinity. This is due to that no channel code is employed for each user.

Since for a given x , $\varphi^{-1}(x)$ is a decreasing function of spreading length L , $\phi(x, \frac{E_b}{N_0}) > \varphi^{-1}(x)$ holds for $x \geq 0$ as L is sufficiently large and $\frac{E_b}{N_0} \rightarrow +\infty$. In this case, the mean of the extrinsic LLR converges to infinity as the number of iteration increases. Due to $\lim_{x \rightarrow +\infty} \phi(x, \frac{E_b}{N_0}) = 4\frac{E_b}{LN_0}$ from Lemma 2, the asymptotic BER of hard decision at the information node in U is estimated as [7]–[10]

$$P_e \approx Q\left(\sqrt{2g(s, L+1)\frac{E_b}{LN_0}}\right) < e^{-\widetilde{g}(s, L)\frac{E_b}{N_0}} \quad (21)$$

where we have used $\varphi(x) \approx g(s, L)x$ as x is large, $Q(x) < e^{-x^2/2}$, and $\widetilde{g}(s, L) \triangleq g(s, L+1)/L$ is referred to as a standard slope. Note that we have used slope $g(s, L+1)$ instead of $g(s, L)$ in (21) since the hard decision is performed based on the total LLR in (7) other than the extrinsic LLR in (5).

In fact as the BER approaches 0, the upper bound in (21) is very tight. Eq. (21) indicates that at the low BER region, the BER curve is approximate to a line with absolute slope $\widetilde{g}(s, L)$. Since $\widetilde{g}(1, L) = 1$ holds for an arbitrary L , at the low BER region, the BER curve of conventional spreading scheme ($s = 1$) always converges to that of (single-user) uncoded BPSK transmission. Unfortunately, this predicament can not be improved by increasing spreading length L . In our work, since $\widetilde{g}(s, L) > 1$ holds for $s, L \geq 2$, the BER curve of finite field spreading with $s, L \geq 2$ has a larger absolute slope than that of single-user transmission with BPSK modulation, and the absolute slope of the BER curve increases as s increases. In addition, there is a special case of $L = 1$, i.e., code rate of each user is 1. It is easy to show that in this case, the BER can never approach 0 for the number of users $K \geq 2$ due to code rate 1 of each user. For single-user ($K = 1$) finite field spreading multiple-access, since $\widetilde{g}(s, 1) \approx 1$ for an arbitrary s , at the low BER region, the absolute slope of the BER curve approaches that of single-user transmission with BPSK modulation.

We verify our analysis above, obtained based on the Gaussian approximation and the approximation of (13), by BER Monte Carlo simulations on practical systems. We consider

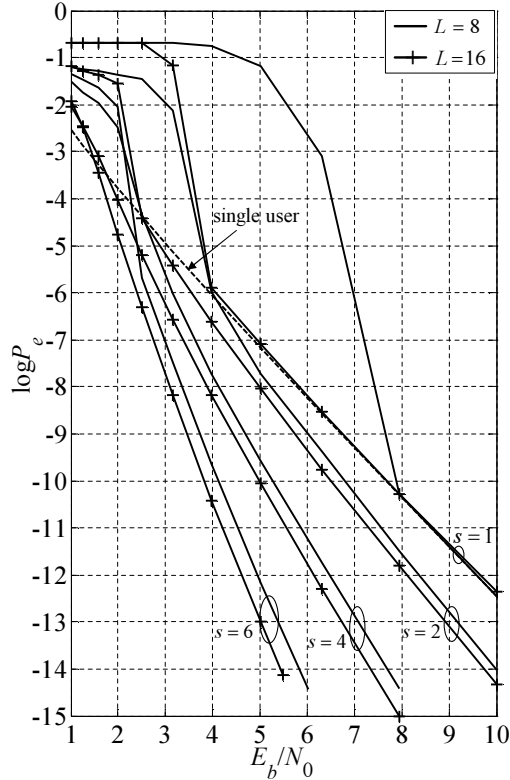


Fig. 5. BER curves of $(K = 8)$ -user finite field spreading multiple-access systems with $L = 8, 16$ and $s = 1, 2, 4, 6$. The information vector length is $sN = 12000$ and the number of decoding iteration is 50.

$(K = 8)$ -user finite field spreading multiple-access system with $L = 8, 16$ and $s = 1, 2, 4, 6$. Fig. 5 illustrates BER curves obtained by Monte Carlo simulations. Since the EXIT function theory is based on the assumption of infinite code length [7]–[10], in our simulations we employ a large code length with the information vector length of $sN = 12000$. The number of decoding iteration is 50. Both mapping $\Gamma(\cdot)$ and the chip-level interleaving are random, and the BER curve illustrates an average BER for all the possible mapping and interleaving realizations. We use horizontal coordinate $\frac{E_b}{N_0}$ and vertical coordinate $\log P_e$ (natural logarithm). We see that at the low BER region, all BER curves are approximate to lines. We compare the absolute slopes of BER curves at low BER region in Fig. 5 with standard slope $\bar{g}(s, L)$ obtained by Theorem 1 in Table I. The difference is less than 0.1 for all the comparison pairs. The two curves for $s = 1$ overlap with each other and converge to the BER curve of single-user transmission with BPSK modulation. Curves for $s \geq 2$ have larger absolute slopes than that of single-user transmission with BPSK modulation. All these phenomenons coincide with our analysis.

TABLE I
COMPARISON BETWEEN ABSOLUTE SLOPES OF BER CURVES AT LOW BER REGION IN FIG. 5 AND $\bar{g}(s, L)$

L	8				16			
s	1	2	4	6	1	2	4	6
BER slope	1.0625	1.2262	1.6364	2.2352	1.0028	1.2373	1.7269	2.3543
$\bar{g}(s, L)$	1	1.2411	1.7002	2.2095	1	1.2675	1.8240	2.4493

VI. CONCLUSIONS

In this paper, we proposed a finite field spreading scheme for the MAC, in which the spreading for multiple bits is performed jointly by the finite field multiplication. Under the iterative decoding, an SINR gain is obtained during the joint spreading. The multi-user finite field spreading multiple-access achieves a lower BER than that of the single-user transmission with BPSK modulation under the iterative decoding.

We considered the finite field spreading multiple-access system without channel coding for each user. If there is a channel code employed as an outer code for each user, our EXIT function analysis of the FF-DES is also available from the theory of concatenated code [8]–[10].

There are still a number of problems in connection with our work that seem to deserve further investigation. In our analysis, we considered an average EXIT function and asymptotic slope for all the mapping and interleaving. In fact, different mapping and interleaving have different EXIT functions that provide different BER performance. Design of spreading and interleaving to achieve better BER performance is an interesting future work.

In the finite field spreading of Fig. 2, every s information bits are spread into L length- s vectors, each of which can be regarded as a codeword of a rate-1 code. These L rate-1 codes constitute a finite field spreading code with rate $\frac{1}{L}$. The L multiplications on finite field can be regarded as L rate-1 encoding operations that determine the L rate-1 codes. These rate-1 encoding can also be realized by other methods, or we can employ codes with rate less than 1 to achieve a better EXIT transfer performance. All these problems deserve further investigations.

APPENDIX A
EXIT FUNCTION OF ESE

Using (1) and (2), the EXIT function of the ESE is derived as

$$\begin{aligned}
E[x_t^{(k)} L^e(x_t^{(k)})] &= E\left[\frac{2\sqrt{\frac{E_b}{L}}x_t^{(k)}\left(y_t - \sqrt{\frac{E_b}{L}}\sum_{i=1, i\neq k}^K \tanh\left(\frac{L^a(x_t^{(i)})}{2}\right)\right)}{\frac{E_b}{L}\sum_{i=1, i\neq k}^K\left(1 - \left(\tanh\left(\frac{L^a(x_t^{(i)})}{2}\right)\right)^2\right) + \frac{N_0}{2}}\right] \\
&= E\left[\frac{2\frac{E_b}{L} + 2\frac{E_b}{L}x_t^{(k)}\sum_{i=1, i\neq k}^K\left(x_t^{(i)} - \tanh\left(\frac{L^a(x_t^{(i)})}{2}\right)\right) + 2\sqrt{\frac{E_b}{L}}x_t^{(k)}z_t}{\frac{E_b}{L}\sum_{i=1, i\neq k}^K\left(1 - \left(\tanh\left(\frac{L^a(x_t^{(i)})}{2}\right)\right)^2\right) + \frac{N_0}{2}}\right] \\
&= E\left[\frac{4}{2\sum_{i=1, i\neq k}^K\left(1 - \left(\tanh\left(\frac{x_t^{(i)}L^a(x_t^{(i)})}{2}\right)\right)^2\right) + L/\frac{E_b}{N_0}}\right] \tag{22} \\
&= E\left[\frac{4}{2\sum_{i=1}^{K-1}\left(1 - \left(\tanh(\tilde{h}_i)\right)^2\right) + L/\frac{E_b}{N_0}}\right] \triangleq \phi\left(m_a, \frac{E_b}{N_0}\right)
\end{aligned}$$

where $\tilde{h}_i, i = 1, \dots, K-1$ are i.i.d. with $\tilde{h}_i \sim \mathcal{N}\left(\frac{m_a}{2}, \frac{m_a}{2}\right)$. Eq. (22) is due to that $x_t^{(k)} \sim \mathcal{U}(\mathcal{X})$ is independent of $x_t^{(i)}, i \neq k$, and z_t . Note that $\phi\left(m_a, \frac{E_b}{N_0}\right)$ is an average EXIT function of the ESE for all the possible transmitted symbols.

We give an upper bound for $\phi\left(m_a, \frac{E_b}{N_0}\right)$

Lemma 2:

$$\phi\left(m_a, \frac{E_b}{N_0}\right) \leq 4\frac{E_b}{LN_0}$$

with equality if $m_a \rightarrow +\infty$. □

Proof: The upper bound is from the fact $|\tanh(x)| \leq 1$. We prove the equality in the upper bound. Let $\frac{1}{2} < p < 1$ be a constant. We have

$$\lim_{m_a \rightarrow +\infty} \phi\left(m_a, \frac{E_b}{N_0}\right) \geq \lim_{m_a \rightarrow +\infty} \frac{4\prod_{i=1}^{K-1} \Pr(\tilde{h}_i \geq m_a - (m_a)^p)}{2\sum_{i=1}^{K-1}\left(1 - \left(\tanh(m_a - (m_a)^p)\right)^2\right) + L/\frac{E_b}{N_0}} \tag{23}$$

$$\begin{aligned}
&\geq \lim_{m_a \rightarrow +\infty} \frac{4\left(1 - \frac{m_a}{2(m_a)^{2p}}\right)^{K-1}}{2\sum_{i=1}^{K-1}\left(1 - \left(\tanh(m_a - (m_a)^p)\right)^2\right) + L/\frac{E_b}{N_0}} \tag{24} \\
&= 4\frac{E_b}{LN_0}
\end{aligned}$$

where (23) is from monotone increasing of $\tanh(x)$ for $x \geq 0$, and (24) is from Chebyshev inequality. Using the squeeze theorem we obtain $\lim_{m_a \rightarrow +\infty} \phi\left(m_a, \frac{E_b}{N_0}\right) = 4\frac{E_b}{LN_0}$. The lemma is proved.

REFERENCES

- [1] A. J. Viterbi “Very low rate convolutional codes for maximum theoretical performance of spread-spectrum multiple-access channels,” *IEEE J. Sel. Areas Commun.*, vol. 8, no. 4, pp. 641-649, May 1990.
- [2] A. J. Viterbi, *CDMA: Principles of Spread Spectrum Communication*, Reading, MA, Addison-Wesley, 1995.
- [3] W. Leung, L. Liu, and P. Li, “Interleaving-based multiple access and iterative chip-by-chip multi-user detection,” *IEICE Trans. Commun.*, vol. E86-B, no. 12, pp. 3634-3637, Dec. 2003.
- [4] P. Li, L. Liu, K. Wu, and W. Leung, “Interleaving-division multiple-access,” *IEEE Trans. Wireless Commun.*, vol. 5, no. 4, pp. 938-947, Apr. 2006.
- [5] K. Li, X. Wang, and P. Li, “Analysis and optimization of interleave-division multiple-access communication systems,” *IEEE Trans. Wireless Commun.*, vol. 6, no. 5, pp. 1973-1983, May 2007.
- [6] G. Song, J. Cheng, and W. Yoichiro, “Spreading and interleaving design for synchronous interleave-division multiple-access,” *IEICE Trans. Fundamentals.*, vol. E95-A, no. 3, pp. 646-656, Mar. 2012.
- [7] S. Y. Chung, T. J. Richardson, and R. L. Urbanke, “Analysis of sum-product decoding of low-density parity-check codes using a Gaussian approximation,” *IEEE Trans. Inf. Theory*, vol. 47, no. 2, pp. 657-670, Feb. 2001.
- [8] S. ten Brink, “Convergence behavior of iteratively decoded parallel concatenated codes,” *IEEE Trans. Commun.*, vol. 49, no. 10, pp. 1727-1737, Oct. 2001.
- [9] T. Richardson and R. Urbanke, *Modern Coding Theory*, Cambridge, Cambridge University Press, 2008.
- [10] W. E. Ryan and S. Lin, *Channel Codes: Classical and Modern*, Cambridge, Cambridge University Press, 2009.
- [11] T. Wo and P. A. Hoeher, “Universal coding approach for superposition mapping,” in *Proc. 6th International Symposium on Turbo Codes and Iterative Information Processing (ISTC 2010)*, pp. 324-328, France, Sept. 2010.
- [12] P. A. Hoeher and T. Wo, “Superposition modulation: myths and facts,” *IEEE Commun. Mag.*, vol. 49, no. 12, pp.110-116, Dec. 2011.